

## **Tumor Uptake of $^{64}\text{Cu}$ -DOTA-Trastuzumab in Patients with Metastatic Breast Cancer**

Joanne E. Mortimer<sup>1</sup>, James R. Bading<sup>1</sup>, Jinha M. Park<sup>2</sup>, Paul H. Frankel<sup>3</sup>, Mary I. Carroll<sup>1</sup>, Tri T. Tran<sup>2</sup>, Erasmus K. Poku<sup>4</sup>, Russell C. Rockne<sup>3</sup>, Andrew A. Raubitschek<sup>4</sup>, John E. Shively<sup>5</sup>, and David M. Colcher<sup>4</sup>

*<sup>1</sup>Department of Medical Oncology and Experimental Therapeutics, City of Hope, Duarte, California; <sup>2</sup>Department of Radiology, City of Hope, Duarte, California; <sup>3</sup>Department of Information Sciences, City of Hope, Duarte, California; <sup>4</sup>Department of Cancer Immunotherapy and Tumor Immunology, Beckman Research Institute of the City of Hope, Duarte, California; <sup>5</sup>Department of Immunology, Beckman Research Institute of the City of Hope, Duarte, California*

### **Corresponding Author:**

Joanne Mortimer, MD

Professor, Department of Medical Oncology & Experimental Therapeutics

City of Hope Comprehensive Cancer Center

1500 East Duarte Road

Duarte, CA 91010

Phone: (626) 256-4673

Fax: (626) 930-5362

E-mail: [jmortimer@coh.org](mailto:jmortimer@coh.org)

**Word count:** 4996

**Acknowledgements of research support:**

DOD grant # BC095002; NCI grant # P30 CA33572

**Running Footline:**

<sup>64</sup>Cu-TRASTUZUMAB UPTAKE IN BREAST CANCER

## ABSTRACT

The goal of this study was to characterize the relationship between tumor uptake of  $^{64}\text{Cu}$ -DOTA-trastuzumab as measured by PET/CT and standard, immunohistochemistry (IHC)-based, histopathologic classification of human epidermal growth factor receptor 2 (HER2) status in women with metastatic breast cancer (MBC). **Methods:** Women with biopsy-confirmed MBC and not given trastuzumab for  $\geq 2$  months underwent complete staging, including  $^{18}\text{F}$ -fluorodeoxyglucose PET/CT. Patients were classified as HER2-positive (HER2+) or negative (HER2-) based on fluorescence *in situ* hybridization (FISH)-supplemented IHC of biopsied tumor tissue. Eighteen patients underwent  $^{64}\text{Cu}$ -DOTA-trastuzumab injection, preceded in 16 cases by trastuzumab infusion (45 mg). PET/CT was performed 21-25 ("Day 1") and 47-49 ("Day 2") h after  $^{64}\text{Cu}$ -DOTA-trastuzumab injection. Radiolabel uptake in prominent lesions was measured as maximum single-voxel standardized uptake value ( $\text{SUV}_{\text{max}}$ ). Average intra-patient  $\text{SUV}_{\text{max}}$  ( $\langle \text{SUV}_{\text{max}} \rangle_{\text{pt}}$ ) was compared between HER2+ and - patients. **Results:** Eleven women were HER2+ (8 IHC 3+, 3 IHC 2+/FISH amplified), while 7 were HER2- (3 IHC 2+/FISH non-amplified; 4 IHC 1+). Median  $\langle \text{SUV}_{\text{max}} \rangle_{\text{pt}}$  (Day 1, Day 2) was (6.6, 6.8 g/ml) for HER 2+ and (3.7, 4.3 g/ml) for HER2- patients ( $P < 0.005$  either day). The distributions of  $\langle \text{SUV}_{\text{max}} \rangle_{\text{pt}}$  overlapped between the two groups, and inter-patient variability was greater for HER2+ than HER2- disease ( $P < 0.005$  and 0.001, respectively, on Days 1 and 2). **Conclusion:** By 1 day after injection, uptake of  $^{64}\text{Cu}$ -DOTA-trastuzumab in MBC is strongly associated with patient HER2 status and is indicative of binding to HER2. The

variability within and among HER2+ patients, as well as the overlap between the HER2+ and HER2- groups, suggests a role for  $^{64}\text{Cu}$ -DOTA-trastuzumab PET/CT in optimizing treatments that include trastuzumab.

**Keywords:** antibody, breast cancer, PET, HER2, clinical trial

Human epidermal growth factor receptor 2 (HER2) is an important target in treatment of breast cancer. Eligibility for HER2-directed therapy is determined from a biopsy of primary or metastatic tumor. Patients whose tumors demonstrate 3+ staining by immunohistochemistry (IHC) or gene amplification by fluorescence *in situ* hybridization (FISH) are considered HER2-positive (HER2+) and are candidates for HER2-directed therapies such as trastuzumab and ado-trastuzumab emtansine (T-DM1) (1). Addition of anti-HER2 treatment to chemotherapy improves patient survival for all stages of HER2+ breast cancer (2).

Because HER2-directed therapies are costly and potentially toxic, it is important to determine which patients are likely to benefit from these treatments. The current selection method is only modestly successful in predicting response or outcome for patients receiving HER2-directed therapy. This is especially true in metastatic breast cancer (MBC), where response rates for first- and second-line treatments are typically 50-80% and 25-50% respectively, and most initial responders experience disease progression within 2 y after starting treatment (3). Furthermore, some HER2-negative (HER2-) patients benefit from anti-HER2 therapy (4).

Several factors limit the predictive accuracy of pathologic HER2 assessment. These assessments are usually based on core needle biopsy of a single lesion and thus may suffer from sampling error due to heterogeneous intra-tumoral distribution of HER2, as well as variable HER2 expression among multiple tumors in the same patient. Furthermore, high HER2 expression or gene amplification does not guarantee efficacy for anti-HER2 therapy. The cancer may have

molecular mechanisms of resistance to the therapeutic agents (5). More fundamentally, response requires that the therapeutic agent(s) be delivered to and incorporated by tumor cells in sufficient quantities. Solid tumors often develop in ways that hinder delivery of blood-borne molecules to tumor cells (6). This is especially true for macromolecules such as antibodies, which distribute from blood into tissue by convection rather than diffusion.

We are developing PET imaging with  $^{64}\text{Cu}$ -DOTA-trastuzumab for the purpose of measuring tumor uptake of trastuzumab in patients with breast cancer. We have shown that  $^{64}\text{Cu}$ -DOTA-trastuzumab PET/CT is highly effective in visualizing tumors in women with HER2+ MBC (n = 8) and that trastuzumab (45 mg) administered prior to  $^{64}\text{Cu}$ -DOTA-trastuzumab decreases hepatic uptake of  $^{64}\text{Cu}$  about 75%, without affecting tumor uptake (7). We report here on our efforts to characterize the relationship between tumor uptake of  $^{64}\text{Cu}$ -DOTA-trastuzumab and standard classification of HER2 status for MBC. For that, we enrolled women with HER2- disease, as well as additional women with HER2+ MBC.

## **MATERIALS AND METHODS**

### **Patient Selection**

Women with MBC outside the breast and regional lymphatics and no exposure to trastuzumab for at least 2 mo were considered for study participation following staging that included  $^{18}\text{F}$ -fluorodeoxyglucose (FDG) PET/CT. All candidates underwent biopsy of a metastatic lesion within 28 d before the  $^{64}\text{Cu}$ -DOTA-trastuzumab procedure to confirm recurrent disease and assess HER2 status.

Immunohistochemical staining was performed on all specimens, and those scored IHC 2+ also underwent FISH. To support accurate PET-derived measurement of  $^{64}\text{Cu}$ -DOTA-trastuzumab uptake in tumors, disease outside the breast/axillary region and biopsy site that measured  $\geq 2.0$  cm was also required. Accrual extended from 3/2011 through 9/2013. The study was approved by the City of Hope Institutional Review Board, and all patients provided written informed consent prior to study participation.

### **$^{64}\text{Cu}$ -DOTA-Trastuzumab Preparation and Administration**

Copper-64 (half-life 12.8 h, 0.18 positrons/decay) was provided by the Mallinckrodt Institute of Radiology, Washington University School of Medicine, St. Louis, MO. Radiolabeled trastuzumab was prepared according to an investigational new drug application (IND #109971). The procedure includes heating at 43°C for 45 min followed by incubation with an excess of DTPA, which eliminates  $^{64}\text{Cu}$  binding to secondary chelating sites on the antibody while maintaining the immunoreactivity of the radiolabeled product (7). The  $^{64}\text{Cu}$ -DOTA-trastuzumab (trastuzumab dose 5 mg) was mixed with saline (25 ml) and administered intravenously (i. v.) over 10 min. Injected radioactivity was 364- 551 MBq (mean 464 MBq). Two patients in the initial study received no additional trastuzumab; the other 16 were given trastuzumab (45 mg) i. v. over 15 min immediately before administration of  $^{64}\text{Cu}$ -DOTA-trastuzumab.

### **PET/CT Imaging**

All images were acquired with the same GE Discovery STe 16 PET/CT scanner (GE Healthcare, Waukesha, WI) operated in 3-D mode (septa retracted). The PET axial field of view is 15.4 cm, with an image slice thickness of 3.3 mm. Consecutive bed positions overlap by 11 slices. The PET images were reconstructed by the iterative, ordered subsets expectation maximization (OSEM) method with Gaussian post-smoothing and standard corrections for scanner dead time, random and scattered coincidence events, non-uniform detector sensitivity and photon attenuation. Spatial resolution of the PET images as measured for an  $^{18}\text{F}$  line source-in-water phantom is 9 mm full-width-at-half maximum.

Patients underwent standard  $^{18}\text{F}$ -FDG PET/CT 1-17 d before the  $^{64}\text{Cu}$ -DOTA-trastuzumab procedure. They fasted  $\geq 6$  h before injection of  $^{18}\text{F}$ -FDG. In all cases, serum glucose concentration met institutional requirements ( $\leq 120$  mg/dl for non-diabetic patients,  $\leq 200$  mg/dl for diabetic patients). Injected activity and time from injection to scan ranged from 407-596 MBq (mean 518 MBq) and 50-72 min, respectively.

Axial coverage in the  $^{64}\text{Cu}$  PET scans was based on tumor location as determined from the preceding  $^{18}\text{F}$ -FDG PET/CT examination. Scan duration for  $^{64}\text{Cu}$  was 60 min, except one scan that was terminated at 40 min due to patient discomfort. To allow accumulation of the radiolabeled antibody in tumor, the first ("Day 1") scan was performed 21-25 h after injection. For all but one patient, a second ("Day 2") scan was obtained 47-49 h post injection. Day 1 scans comprised 3 or 4 bed positions (20 or 15 min each) and Day 2 scans 1 or 2 bed positions (60 or 30 min each), depending on patient body thickness. Multiple bed positions were



acquired contiguously, except for 2 patients for whom the scans were made partially discontinuous to increase disease coverage.

### **Image Analysis**

Scans were interpreted by an expert radiologist (JP). Tumors and other anatomic features were considered PET-positive if visualized with positive contrast relative to adjacent tissue. Lesion-like, PET-positive findings were disregarded if CT was judged inconclusive.

Image analysis was performed with XD version 3.6 (Mirada Medical; Oxford, England). Radiolabel uptake for tumors was measured in terms of single-voxel maximum standardized uptake value ( $SUV_{max}$ ;  $SUV = \text{tissue activity per ml} \times \text{body weight (g)} / \text{injected activity decay-corrected to time of scan}$ ). A detailed description of the criteria used in judging the suitability of tumor images for measurement of  $SUV_{max}$ , as well as the methods used to define the volumes of interest (VOIs) within which  $SUV_{max}$  was determined, is provided in the supplemental material (available at <http://jnm.snmjournals.org>). In brief,  $SUV_{max}$  was measured for lesions that were identifiable on CT and for which the PET maximum voxel was (a) clearly associated with the CT correlate, and (b) not overlapped by the image of an adjacent PET-positive feature (vessel, organ, tumor, etc.). The number of lesions evaluated per patient was limited to 10. Measurements excluded the 2 transaxial slices at either end of a scan, where random noise tends to be excessive due to low detection sensitivity. Biopsied tumors were excluded *a priori* from the analysis due to possible effect of the biopsy procedure on radiotracer uptake. [The data

suggest higher uptake in biopsied tumors. Conclusions were not altered when the biopsy sites were included in the analysis (data not shown). ]

Measurements of  $^{64}\text{Cu}$  activity in blood were obtained from PET images of the cardiac ventricles. Mean SUVs were determined for regions of interest of fixed size placed well within the ventricle boundaries on 3 contiguous transaxial image slices.

Tumor size was estimated from  $^{18}\text{F}$ -FDG images. Volumes of interest were defined for those images using a maximum voxel-based thresholding technique (8), with the 3-D isocontour tailored to approximate the boundary of the tumor CT image. Details of the analysis are given in the supplemental material.

### **Statistical Analysis**

The study was designed to accrue at least 8 HER2+ and 7 HER2- patients. This plan provided 80% power to detect an effect = 1.36 x the common standard deviation of  $\text{SUV}_{\text{max}}$  with a one-sided significance level of 0.05 when comparing  $^{64}\text{Cu}$ -DOTA-trastuzumab uptake between the HER2+ and - groups. The actual accrual of HER2+ patients was 11 during the course of enrolling 7 HER2- patients, resulting in greater-than-planned power.

We used mean intra-patient  $\text{SUV}_{\text{max}}$  ( $\langle\text{SUV}_{\text{max}}\rangle_{\text{pt}}$ ) as the primary metric for patient-level comparisons. We also compared uptake between the HER2+ and - groups treating  $\text{SUV}_{\text{max}}$  measurements for individual tumors as independent observations. Because they are skewed, we characterized  $\langle\text{SUV}_{\text{max}}\rangle_{\text{pt}}$  and  $\text{SUV}_{\text{max}}$  distributions in terms of median rather than mean values. Statistical

significance of differences in  $\langle \text{SUV}_{\text{max}} \rangle_{\text{pt}}$  and  $\text{SUV}_{\text{max}}$  between patient groups was assessed via a non-parametric (Wilcoxon rank sum) test.

We also compared inter- and intra-patient variability of tumor uptake of  $^{64}\text{Cu}$ -DOTA-trastuzumab between the HER2+ and – groups. The coefficient of variation (CV) for  $\langle \text{SUV}_{\text{max}} \rangle_{\text{pt}}$  was compared using both an F-test and a Wilcoxon rank sum test. The Wilcoxon test was used to compare intra-patient CVs of  $\text{SUV}_{\text{max}}$  between the 2 patient groups. Linear models were used to consider the effect of lesion site.

All significance testing was 2-sided, with  $P < 0.05$  considered statistically significant.

## RESULTS

### Patients

Participating patients are described in Table 1. The HER2+ group ( $n = 11$ ) includes the 8 women from our initial feasibility study (7). The HER2+ and – groups are closely similar with regard to age and hormone receptor status. Of the 8 women with HER2+ disease previously treated with trastuzumab, time between the last dose of the antibody and  $^{64}\text{Cu}$ -DOTA-trastuzumab injection was 11 wk for one and at least 4 mo for all the others. Anatomic distribution of tumors for which uptake was measured was proportionately similar for HER2+ vs. HER2- patients, with the biggest difference being 6 vs. 0 liver metastases. Tumors were, on average, larger for HER2- than HER2+ patients. However,  $\text{SUV}_{\text{max}}$  for  $^{64}\text{Cu}$ -DOTA-trastuzumab was not significantly related to tumor size for either group (Supplemental Fig. 1).

### Tumor Uptake of $^{64}\text{Cu}$ -DOTA-trastuzumab

Tumor uptake data are plotted in Fig. 1. The number of lesions evaluated for Days 1 and 2 were 58 and 46 for HER2+ patients, versus 29 and 18 for HER2- patients. For a given patient, the axial range of the scan was shortened between Day 1 and 2, in general reducing the number of lesions evaluated on Day 2. Some lesions were evaluable only on Day 2 because of technical error or insufficient lesion-to-background contrast on Day 1. One patient in the IHC1+ subgroup was not able to undergo scanning on Day 2 and 1 patient in the IHC2+/FISH- group had no lesions that were evaluable for  $\text{SUV}_{\text{max}}$  on Day 1.

Tumor uptake of  $^{64}\text{Cu}$ -DOTA-trastuzumab was, on average, higher in HER2+ than in HER2- patients, regardless of whether the data for individual lesions were grouped by patient (Fig. 1, parts A and C) or treated as independent observations (Fig. 1, parts B and D). On Day 1, median  $\langle\text{SUV}_{\text{max}}\rangle_{\text{pt}}$  was 6.6 [interquartile range (IQR) 5.6-9.5] g/ml for the HER2+ group versus 3.7 (IQR 3.3-4.1) g/ml for the HER2- group ( $P < 0.005$ ). On Day 2, the corresponding values were 6.8 (IQR 6.0-9.4) and 4.3 (IQR 4.1-4.9) g/ml ( $P < 0.005$ ). For individual tumors, median  $\text{SUV}_{\text{max}}$  for HER2+, - patients was 7.0 (IQR 4.8-10.6), 3.7 (IQR 3.0-4.7) g/ml on Day 1 ( $P < 0.001$ ), and 8.7 (IQR 5.7-13.0), 4.6 (IQR 3.8-5.0) g/ml on Day 2 ( $P < 0.001$ ). Within the HER2+ and - classifications, differences in  $\langle\text{SUV}_{\text{max}}\rangle_{\text{pt}}$  and  $\text{SUV}_{\text{max}}$  distributions between any of the positive IHC/FISH subgroups and any of the negative IHC/FISH subgroups were all significant, and IHC 1+ was lower than IHC 2+/FISH- ( $P < 0.05$ , Wilcoxon Test).

Tumor uptake and tumor-to-non-tumor contrast generally increased between Day 1 and 2 for both HER2+ and – patients (Fig. 2). For lesions measured both days,  $SUV_{max}$  was higher ( $P < 0.001$ , t-Test) on Day 2 than Day 1 for 33 of 38 (87%) tumors in HER2+ patients [average % change  $27 \pm 24$  (mean  $\pm$  SD)] and 13 of 14 (93%) tumors in HER2- patients (average % change  $36 \pm 26$ ), even as blood SUV decreased by  $26 \pm 9\%$  and  $18 \pm 4\%$ , respectively, in the 2 groups.

Tumor uptake varied more among and within HER2+ than HER2- patients (Fig. 1). The variance of  $\langle SUV_{max} \rangle_{pt}$  was 30-fold greater for HER2+ than HER2- patients on Day 1 ( $P < 0.005$ ) and 56-fold greater on Day 2 ( $P < 0.001$ ). For patients with  $> 1$  measured lesion, intra-patient CVs for  $SUV_{max}$  were  $40 \pm 15\%$  (mean  $\pm$  SD) and  $32 \pm 15\%$ , respectively, for HER2+ and – patients on Day 1 ( $P = NS$ ),  $37 \pm 16\%$  and  $20 \pm 2\%$  on Day 2 ( $P < 0.05$ ).

The  $\langle SUV_{max} \rangle_{pt}$  and  $SUV_{max}$  distributions for HER2+ and - patients overlapped substantially (Fig. 1). For Days 1 and 2, respectively, 1 and 3 patients classified as HER2+ had lower  $\langle SUV_{max} \rangle_{pt}$  than the highest patient classified as HER2-. On Days 1 and 2, respectively, 47 and 43% of the  $SUV_{max}$  measurements for the HER2+ group were  $<$  the highest  $SUV_{max}$  value for the HER2- group.

Overlap of the uptake distributions for the HER2+ and – groups is exemplified in Fig. 3, in which images of a HER2+ patient (IHC 3+) and a HER2- patient (IHC 1+) are compared. Both had lesions at or near the surface of a breast that were well visualized by PET/CT 1 d after injection of  $^{64}Cu$ -DOTA-trastuzumab and for which  $SUV_{max}$  was similar.

### **Tumor uptake compared between $^{64}\text{Cu}$ -DOTA-trastuzumab and $^{18}\text{F}$ -FDG**

There was no significant difference in tumor uptake of  $^{18}\text{F}$ -FDG between HER2+ and – patients [median  $\langle\text{SUV}_{\text{max}}\rangle_{\text{pt}}$  8.5 (IQR 6.6-10.9) and 8.7 (IQR 5.4-10.7) g/ml, respectively]. Neither same-lesion ( $\text{SUV}_{\text{max}}$ ) nor same-patient ( $\langle\text{SUV}_{\text{max}}\rangle_{\text{pt}}$ ) uptake was correlated between  $^{18}\text{F}$ -FDG and  $^{64}\text{Cu}$ -DOTA-trastuzumab.

### **DISCUSSION**

The half-life of  $^{64}\text{Cu}$  (13 h) is short relative to the pharmacokinetics of antibodies. However, for  $^{64}\text{Cu}$ -DOTA-trastuzumab in MBC, our observations show that most tumors are well visualized with PET and uptake is indicative of binding to HER2 within 1 d post injection, even in patients classified as HER2-. [Note that all patients in the study had at least low-level (IHC 1+) expression of HER2 in a biopsied tumor.] Measured tumor uptake was positively correlated with patient HER2 status as defined by ASCO-CAP guidelines (1). Furthermore,  $\text{SUV}_{\text{max}}$  increased between Day1 and Day 2 for the preponderance of tumors measured on both days.

It is generally agreed that tumor uptake is best measured after most of the radiotracer has left the blood, at which time uptake is near maximal and most accurately reflects binding to the molecular target (9). For antibodies, such “late-phase” imaging necessitates a radiolabel half-life  $\geq$  several days, leading some investigators to prefer  $^{89}\text{Zr}$  ( $t_{1/2} = 3.3$  d) as the PET radiolabel.

Several clinical investigations with  $^{89}\text{Zr}$ -trastuzumab in MBC have been reported. Gebhart, et al., (10) grouped 56 HER2+ patients according to the proportion of FDG-avid tumors showing  $^{89}\text{Zr}$ -trastuzumab uptake > blood pool activity. Their findings (29% negative, 25% positive, 46% heterogeneous) are similar to our observations with  $^{64}\text{Cu}$ -DOTA-trastuzumab in HER2+ patients (Fig. 1C, details in supplemental material). Ulaner, et al., (11) measured  $\text{SUV}_{\text{max}}$  in 9 patients with HER2- primary tumors. Five tumors (each in a different patient) were positively imaged with  $^{89}\text{Zr}$ -trastuzumab;  $\text{SUV}_{\text{max}}$  values for those are consistent with ours (details in supplemental material). Interestingly, only the 2 tumors with lowest  $\text{SUV}_{\text{max}}$  were HER2+ on subsequent histopathology, thus demonstrating that trastuzumab uptake is not equivalent to HER2 expression.

Our work implies that trastuzumab binding in MBC is sufficiently rapid that visualization and measurement of HER2-specific uptake can be achieved for most tumors within 1-2 d post injection. This is significant for PET imaging of trastuzumab with respect to both patient radiation dose and clinical applicability. The radiation dose necessary to obtain good-quality tumor images and uptake measurements may be much lower with the shorter-lived  $^{64}\text{Cu}$  radiolabel (7, 12). However, this results from being able to image effectively at 1-2 d, rather than from the difference in radioisotope decay rates. If the disease burden is unlikely to be obscured by activity in adjacent blood vessels,  $^{89}\text{Zr}$ -trastuzumab PET/CT can also be performed 1-2 d post injection, with concomitant reduction of injected activity. Furthermore, a shorter examination period is a significant advantage in the context of patient treatment schedules.

We observed large variability in tumor uptake of  $^{64}\text{Cu}$ -DOTA-trastuzumab both among and within patients. We previously showed that, in MBC,  $^{64}\text{Cu}$ -DOTA-trastuzumab  $\langle \text{SUV}_{\text{max}} \rangle_{\text{pt}}$  is linearly correlated with average number of HER2 gene copies/tumor cell ( $\langle \# \text{ HER2 copies/cell} \rangle_{\text{pt}}$ ) as measured by FISH, and that the wide range of  $^{64}\text{Cu}$ -DOTA-trastuzumab uptake among HER2+ patients (5-fold in the current study) likely reflects variation in tumor HER2 expression driven by gene amplification (13). However, HER2 expression does not fully explain the observed heterogeneity, given that some patients have substantially higher  $\langle \text{SUV}_{\text{max}} \rangle_{\text{pt}}$  than others with lower  $\langle \# \text{ HER2 copies/cell} \rangle_{\text{pt}}$ . Patients might be misclassified due to biopsy sampling error resulting from heterogeneous intra-tumoral distribution of HER2. Similarly, intra-patient heterogeneity of  $^{64}\text{Cu}$ -DOTA-trastuzumab uptake (up to 5-fold in the current study) might result from variable HER2 expression among different tumors. However, the existing evidence indicates a low incidence of intra-tumoral and intra-patient heterogeneity of HER2 expression (14, 15). Physiologic barriers against antibody delivery to cells within solid tumors have been well-documented in xenografted models (6), but their clinical importance remains largely unexplored.

One way of investigating the role of physiologic barriers is to examine the lesion site dependence of trastuzumab uptake (Supplemental Fig. 2). Unfortunately, our study is not fully representative of the anatomic sites of MBC. None of the patients had active metastasis to brain and only 3 patients (all HER2+) had evaluable liver metastases (6 in total). Although the data suggest higher uptake in the liver lesions,



there were no statistically significant differences among lesion sites for either HER2+ or HER2- patients.

Measurement error contributes variability and bias to PET measurements of radiopharmaceutical uptake. In particular, the “partial volume effect” (PVE) causes negative bias with magnitude inversely related to object size (8). In the current study, evaluated lesions were, on average, larger for the HER2- than the HER2+ patients (Supplemental Fig. 1). However, the PVE would have tended to decrease values measured in HER2+ relative to HER2- patients. Thus, its potential influence does not detract from the conclusion that, on average, tumor uptake of the antibody was higher in the HER2+ compared with the HER2- group.

Whatever the cause(s), the observed heterogeneity in tumor uptake of the radiolabeled antibody implies a potential role for  $^{64}\text{Cu}$ -DOTA-trastuzumab PET/CT in patient selection and treatment design for therapy that includes trastuzumab. The variability in uptake seen among women with HER2+ MBC is reminiscent of the limited rates of response in such patients (3), while the observation that uptake in some HER2- patients exceeded that in some HER2+ patients is consistent with the fact that some HER2- patients benefit from treatment with trastuzumab (4). The point is that, unlike histopathology,  $^{64}\text{Cu}$ -DOTA-trastuzumab PET/CT measures trastuzumab dose to tumor following intravenous administration and, therefore, may improve prediction of response to and benefit from the antibody over histopathology alone. Furthermore, individualized treatment design could be enabled by measurement of trastuzumab uptake at different sites of metastasis within a single patient.

A key question not addressed in the current study is whether tumor uptake of  $^{64}\text{Cu}$ -DOTA-trastuzumab is actually correlated with tumor response or patient benefit. Trastuzumab is usually combined with chemotherapy, obscuring the effects of the antibody. For the antibody-drug conjugate T-DM1 on the other hand, uptake of trastuzumab is the primary determinant of therapeutic dose to tumor. Others have shown that tumor uptake of  $^{89}\text{Zr}$ -trastuzumab, assessed by qualitative inspection of PET/CT images, is highly accurate in predicting early response to T-DM1 in HER2+ MBC (10). We are currently evaluating  $^{64}\text{Cu}$ -DOTA-trastuzumab PET/CT for prediction of response and benefit for women receiving T-DM1 as second-line treatment for HER2+ MBC. A question explored in that study is whether a threshold for tumor uptake of  $^{64}\text{Cu}$ -DOTA-trastuzumab can be established below which the likely benefit from T-DM1 therapy is no greater than from alternative treatments.

## **CONCLUSION**

Uptake of  $^{64}\text{Cu}$ -DOTA-trastuzumab in metastatic breast cancer was strongly associated with patient HER2 status by 1 d after injection and increased between Days 1 and 2 in most tumors for both HER2+ and - patients. These observations imply that  $^{64}\text{Cu}$ -DOTA-trastuzumab uptake in MBC is indicative of binding to HER2 within 24 h post injection. Tumor uptake varied widely among and within patients classified as HER2+, and the distributions of intra-patient average and individual tumor  $\text{SUV}_{\text{max}}$  overlapped substantially between HER2+ and HER2- patients. This

suggests a role for  $^{64}\text{Cu}$ -DOTA-trastuzumab PET/CT in optimizing treatments that include trastuzumab.

## **DISCLOSURE**

J. E. Mortimer is a consultant for Puma Pharmaceuticals. This study was funded by Department of Defense Grant # BC095002 (J. M. Mortimer, Principal Investigator). The production of  $^{64}\text{Cu}$  at Washington University School of Medicine is supported by the Department of Energy. Research reported in this publication included work performed in the City of Hope Clinical Pathology and Biostatistics Cores supported by the National Cancer Institute of the National Institutes of Health under award number P30CA033572. The content is solely the responsibility of the authors and does not necessarily represent the official views of the National Institutes of Health.

## **ACKNOWLEDGMENTS**

Image analysis utilized customized software provided by Mirada Medical, Oxford, England. The authors especially thank Mirada Medical U.S. Support Manager Jennifer Miller for her assistance in implementing and maintaining the software.

## REFERENCES

1. Wolff AC, Hammond MEH, Hicks DG, et al. Recommendations for human epidermal growth factor receptor 2 testing in breast cancer: American Society of Clinical Oncology/College of American Pathologists clinical practice guideline update. *J Clin Oncol* 2013;31:3997-4013.
2. Giordano SH, Temin S, Kirshner JJ, et al. Systemic therapy for patients with advanced human epidermal growth factor receptor 2–positive breast cancer: American Society of Clinical Oncology clinical practice guideline. *J Clin Oncol* 2014;32:2078-2099.
3. Nielsen DL, Kümler I, Palshof AE, Andersson M. Efficacy of HER2-targeted therapy in metastatic breast cancer: monoclonal antibodies and tyrosine kinase inhibitors. *The Breast* 2013;22:1-12.
4. Pogue-Geile KL, Kim C, Jeong J-H, et al. Predicting degree of benefit from adjuvant trastuzumab in NSABP trial B-31. *J Natl Cancer Inst* 2013;105:1782-1788.
5. Singh JC, Jhaveri K, Esteva FJ. HER2-positive advanced breast cancer: optimizing patient outcomes and opportunities for drug development. *Br J Cancer* 2014;111:1888-1898.
6. Jain R. Delivery of molecular and cellular medicine to solid tumors. *Adv Drug Deliv Rev* 2012;64(Suppl):353-365.
7. Mortimer JE, Bading JR, Colcher DM, et al. Functional imaging of human epidermal growth factor receptor 2–positive metastatic breast cancer using

- <sup>64</sup>Cu-DOTA-trastuzumab PET. *J Nucl Med* 2014;55:23-29.
8. Boellaard R, Krak NC, Hoekstra OS, Lammertsma AA. Effects of noise, image resolution, and ROI definition on the accuracy of standard uptake values: a simulation study. *J Nucl Med* 2004;45:1519-1527.
  9. Van Dongen GAMS, Visser GM, Lub-de Hooge MN, Vries EG, Perk LR. Immuno-PET: a navigator in monoclonal antibody development and applications. *The Oncologist* 2007;12:1379-1389.
  10. Gebhart G, Lamberts LE, Wimana Z, et al. Molecular imaging as a tool to investigate heterogeneity of advanced HER2-positive breast cancer and to predict patient outcome under trastuzumab emtansine (T-DM1): the ZEPHIR trial. *Annals of Oncology* 2016;27:619-624.
  11. Ulaner GA, Hyman DM, Ross, DS, et al. Detection of HER2-positive metastases in patients with HER2-negative primary breast cancer using <sup>89</sup>Zr-Trastuzumab PET/CT. *J Nucl Med* 2016;57:1523-1528.
  12. LaForest R, Lapi SE, Oyama R, et al. [<sup>89</sup>Zr]Trastuzumab: evaluation of radiation dosimetry, safety, and optimal imaging parameters in women with HER2-positive breast cancer. *Mol Imaging Biol* 18:952-959.
  13. Bading J, Press M, Villalobos I, et al. Tumor uptake of <sup>64</sup>Cu-DOTA-trastuzumab correlates with HER2 gene amplification in patients with metastatic breast cancer. *J Nucl Med* 2016;57(Suppl 2):25P.
  14. Rossi S, Basso M, Strippoli A, et al. Hormone receptor status and HER2 expression in primary breast cancer with synchronous axillary metastases or recurrent metastatic disease. *Clin Breast Cancer* 2015;15:307-312.

15. Allott EM, Geradts J, Sun X, et al. Intratumoral heterogeneity as a source of discordance in breast cancer biomarker classification. *Breast Cancer Res* 2016;18:68.

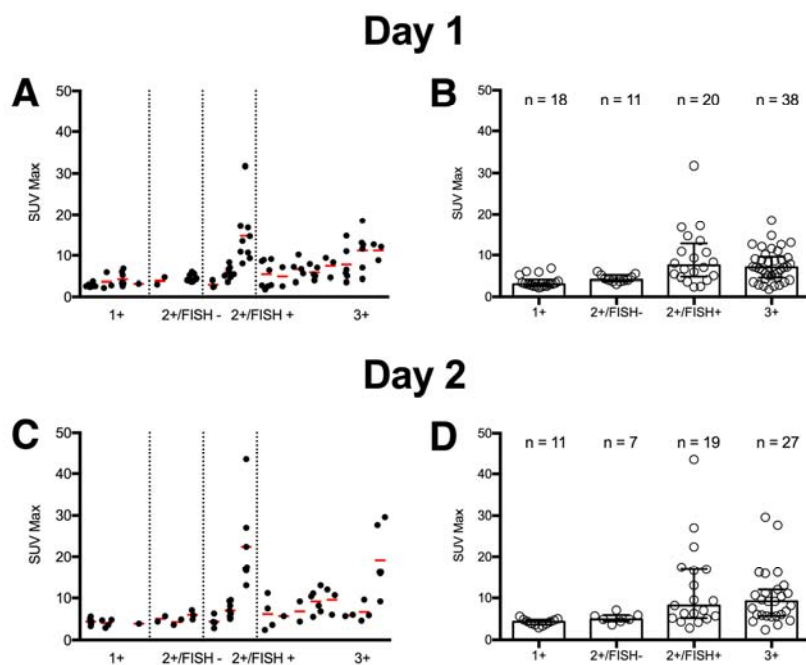


**FIGURE 1.** Tumor uptake ( $SUV_{max}$ ) of  $^{64}\text{Cu}$ -DOTA-trastuzumab versus patient IHC/FISH score from biopsied tumor. Data are from  $^{64}\text{Cu}$ -DOTA-trastuzumab PET/CT scans acquired 1 day (A, B) and 2 days (C, D) post injection. In A and C, the data for individual tumors (black dots) are grouped by patient and IHC/FISH score. Intra-patient means are represented by red horizontal lines. In B and D,  $SUV_{max}$  values for individual lesions (open circles) are combined across patients and grouped by IHC/FISH score ( $n$  = number of tumors per group). Intra-group medians are represented as amplitudes of rectangular overlays; errors bars denote 1<sup>st</sup> and 3<sup>rd</sup> quartiles. In both analyses, tumor uptake is generally higher for the HER2+ subgroups (3+ or 2+/FISH+) ( $P < 0.005$ ). Relative variability of uptake was greater for the HER2+ than the HER2- group, both among ( $P < 0.001$ ) and within ( $P < 0.05$  on Day 2) patients.



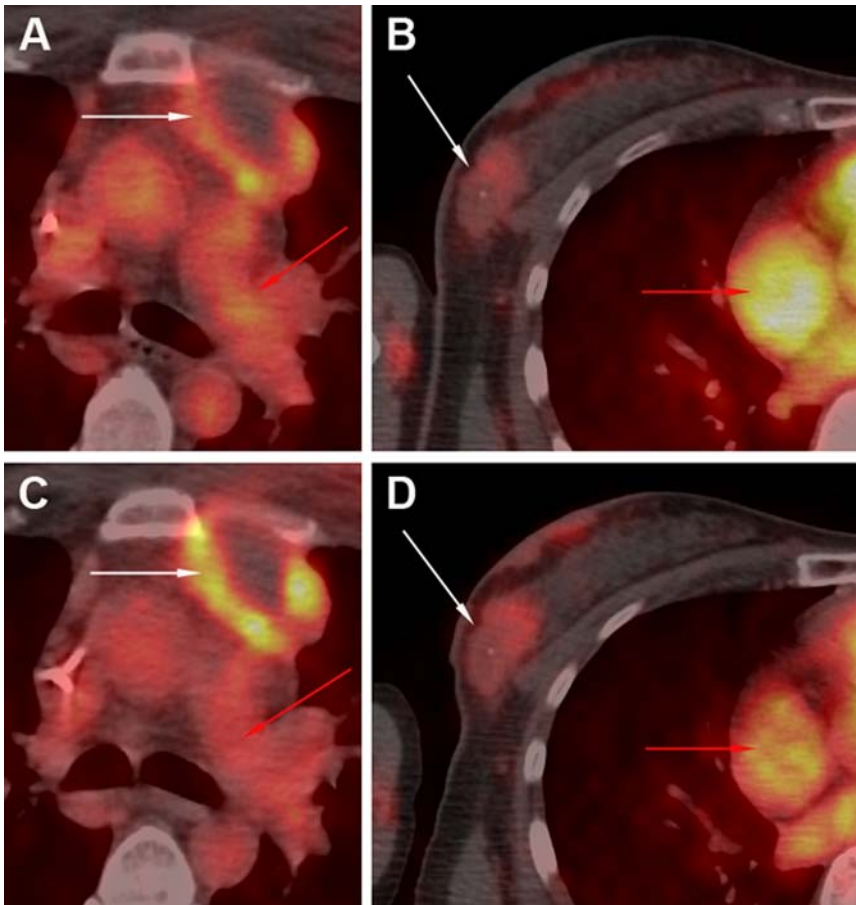


**FIGURE 2.** Examples of increased tumor uptake and tumor-to-non-tumor contrast between 1 and 2 days after injection of  $^{64}\text{Cu}$ -DOTA-trastuzumab. White and red arrows respectively denote tumors and blood pool as seen in transaxial PET/CT fusion images. The images on the left are from a HER2+ (IHC2+/FISH+) patient. Panels A (Day 1) and C (Day 2) show a large metastasis in a pre-vascular lymph node for which uptake was concentrated at the tumor surface. The upper intensity threshold (white color) corresponds to SUV = 22 g/ml. At the times of the 2 scans (24 and 48 h), measured SUV<sub>max</sub> for the tumor was 17 and 27 g/ml, respectively, while the SUV for blood was 15 and 11 g/ml. The right-hand column depicts a metastatic mass in the right breast of a HER2-negative patient (IHC1+). The upper intensity threshold for the images (white color) was set at SUV = 10 g/ml. The

SUV<sub>max</sub> for the tumor increased from 2.6 to 5.0 g/ml between (B) the Day 1 (25 h post-injection) and (D) the Day 2 (49 h post injection) scan, while the SUV for blood declined from 12 to 8.8 g/ml.

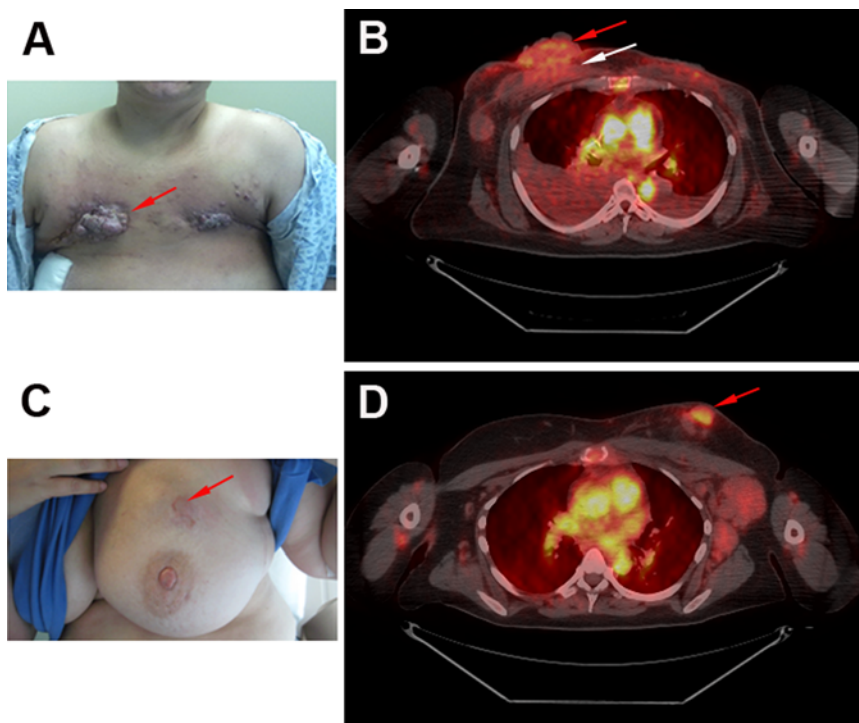


**FIGURE 3.** Examples of tumor visualization with  $^{64}\text{Cu}$ -DOTA-trastuzumab PET/CT. The scan images are transaxial PET/CT fusion images with upper intensity thresholds (white color) corresponding to  $\text{SUV} = 10 \text{ g/ml}$ . The patient depicted in (A) and (B) had recurrent disease following double mastectomy that was scored IHC 1+. The scan began 21 h post injection. Measured  $\text{SUV}_{\text{max}}$  was 6.9 g/ml for the lesion in the surface of the right breast (red arrow) and 6.0 g/ml for the mass beneath it (white arrow). The patient shown in (C) and (D) had widespread metastatic disease scored as IHC 3+. The scan, begun 25 h after injection, showed an  $\text{SUV}_{\text{max}}$  of 7.0 g/ml in a tumor at and near the surface of the left breast (arrows).

**TABLE 1**  
Patient Demographics and Clinical Characteristics

	Age (years)			Hormone receptor and HER2 status of recurrent disease (# of patients)							
	No. of patients	median	range	ER & PR receptors		HER2					
				ER &/or PR positive	ER & PR negative	IHC1+	IHC2+	IHC3+			
HER2+	11	59	35-75	6	5			3	8		
HER2-	7	61	40-71	3	4	4		3			

	Prior anti-HER2 therapy		Sites of metastatic disease measured for SUV <sub>max</sub>						Tumor volume (cm <sup>3</sup> )*	
	none	trastuzumab for metastasis	bone	lymph nodes	liver	lung	other <sup>†</sup>	breast /chest wall <sup>‡</sup>	mean	SE
HER2+	3	8 (79 d-36 mo)	24	23	6	6	2	5	5.8	0.9
HER2-	7		12	10	0	3	3	5	12.2	2.7

\*Volume within isocontour of <sup>18</sup>F-FDG tumor image approximately matching boundary of CT correlate

<sup>†</sup>Pulmonary effusion (HER2+) or body wall outside breast region

<sup>‡</sup>Breast or chest wall adjacent to breast

HER2 = human epidermal growth factor receptor 2; ER = estrogen receptor; PR = progesterone receptor; IHC = immunohistochemistry; SE = standard error

## MATERIALS AND METHODS

### Image Analysis

**Lesion selection.** Tumors and non-tumor anatomic features (vessels, organs, etc.) were considered PET-positive if they were visualized on PET with positive contrast relative to adjacent tissue. Radiolabel uptake was measured for tumors (a) that were identifiable on CT and (b) whose PET images were not obscured by overlap with the PET image of an adjacent PET-positive feature.

**Uptake measurements, overview.** PET image intensity or brightness was calibrated in units of radiolabel activity concentration based on scans of a large cylindrical phantom filled with a known, uniform concentration of  $^{18}\text{F}$ . Radiolabel uptake in tissue was measured in terms of maximum voxel standardized uptake value ( $\text{SUV}_{\text{max}}$ ), where “maximum voxel” refers to the voxel with maximum intensity within a given volume of interest (VOI). Once a VOI was defined, the software automatically indicated the location of the maximum voxel and calculated  $\text{SUV}_{\text{max}}$ .

**Uptake measurements,  $^{18}\text{F}$ -FDG.** Analysis for a given tumor began with the  $^{18}\text{F}$ -FDG scan. The  $^{18}\text{F}$ -FDG tumor images were segmented via a maximum voxel-based thresholding (MVBT) technique (1). For a given lesion, a 3-dimensional rectangular VOI (threshold setting = 0% of maximum) was defined which contained the tumor image as identified by the study radiologist. The rectangular VOI was adjusted as needed to bring the maximum voxel within the tumor CT image. The PET images were inspected to determine whether the maximum voxel was overlapped by the PET-positive image of an adjacent feature. If not,  $\text{SUV}_{\text{max}}$  and the transaxial slice number for the maximum voxel were recorded. In practice, there were no instances in which a measurement of  $\text{SUV}_{\text{max}}$ (FDG) was rejected.

There were 2 tumors for which the rectangular VOI could not be adjusted to bring the maximum voxel within the tumor CT image while simultaneously encompassing the entire  $^{18}\text{F}$ -FDG tumor image. For those lesions, the VOI was divided into 2 contiguous axial segments which together included the entire tumor PET image, and for which the maximum voxel for each segment lay within the tumor CT image. The largest value of  $\text{SUV}_{\text{max}}(\text{FDG})$  for the combined segments was recorded.

**Uptake measurements,  $^{64}\text{Cu}$ -DOTA-trastuzumab.** Patients underwent a PET/CT scan approximately 24 h after injection of  $^{64}\text{Cu}$ -DOTA-trastuzumab (“Day 1” scan); all but 1 of the 18 patients had a second PET/CT scan approximately 48 h post injection (“Day 2” scan).

Alignment among the  $^{18}\text{F}$ -FDG and  $^{64}\text{Cu}$ -DOTA-trastuzumab PET/CT scans was optimized for each tumor. The CT scans were automatically coregistered via a rigid-body technique. The axial alignments of the  $^{64}\text{Cu}$  PET/CT scans were then adjusted to maximize visual similarity of the tumor CT images with the tumor CT image for the  $^{18}\text{F}$  scan. Corresponding slice numbers from the optimally-aligned scans were recorded to facilitate subsequent review.

The coregistered  $^{64}\text{Cu}$ -DOTA-trastuzumab images were inspected in the region of the tumor CT image. If the maximum  $^{64}\text{Cu}$  intensity in that region was clearly influenced by an adjacent feature, the tumor was recorded as non-measurable for uptake of  $^{64}\text{Cu}$ -DOTA-trastuzumab.

For tumor  $^{64}\text{Cu}$ -DOTA-trastuzumab images that were not rejected, the next step was to determine if the tumor image could be segmented by the same 3-D rectangular box, MVBT technique used for  $^{18}\text{F}$ -FDG. If so,  $\text{SUV}_{\text{max}}$  [denoted  $\text{SUV}_{\text{max}}(\text{tras})$ ] was determined

by a procedure analogous to that used for  $^{18}\text{F}$ -FDG, including the requirement that the measurements not appear to be influenced by adjacent, PET-positive features. For the 2 tumors for which the FDG VOI comprised 2 axial segments, the trastuzumab VOIs were constructed as 2 contiguous axial segments matching those of the coregistered FDG VOI. There were also 1 other trastuzumab Day 1 tumor image and 2 other trastuzumab Day 2 tumor images for which 2 axial segments were required in order to bring the maximum voxel within the tumor CT image. In addition, there was 1 trastuzumab Day 2 tumor image that required 3 axial segments. In total, the 3-D rectangular box, MVBT technique was used to evaluate  $\text{SUV}_{\text{max}}(\text{tras})$  for 78 of 87 Day 1 tumor images and 61 of 64 Day 2 tumor images.

Some  $^{64}\text{Cu}$ -DOTA-trastuzumab tumor images (9 Day 1 and 3 Day 2) could not be segmented by the 3-D rectangular box, MVBT technique because of low tumor uptake relative to adjacent features. In those cases, the MVBT technique was used to define a VOI for the tumor  $^{18}\text{F}$ -FDG image that approximately matched the boundary of the tumor CT image. The VOI for the tumor  $^{64}\text{Cu}$ -DOTA-trastuzumab image was then drawn slice-by-slice on transaxial images to match the corresponding FDG isocontours with respect to size, shape and relationship to the tumor CT image, and  $\text{SUV}_{\text{max}}(\text{tras})$  was evaluated for that VOI. One patient had two intra-hepatic tumors that were visualized with  $^{18}\text{F}$ -FDG but whose  $^{64}\text{Cu}$ -DOTA-trastuzumab images appeared equally intense with adjacent liver. For those,  $\text{SUV}_{\text{max}}(\text{tras})$  was equated with the mean SUV for  $^{64}\text{Cu}$ -DOTA-trastuzumab within the FDG-matched VOI.

**Uptake measurements, special case.** Random, count-dependent noise can be excessive near the ends of the axial range of a PET scan. Because of that, our SUV

measurements excluded the final 2 slices at either end of a scan. In no instance did the  $^{18}\text{F}$ -FDG image of an evaluated tumor extend into the final 2 slices. For  $^{64}\text{Cu}$ -DOTA-trastuzumab, however, the lesion extended into or beyond the final 2 slices for 7 of the 151 tumor images evaluated. In those cases, the SUV measurements employed VOIs for  $^{64}\text{Cu}$ -DOTA-trastuzumab and  $^{18}\text{F}$ -FDG that excluded the portion of the tumor that extended into or beyond the 2 end slices of the  $^{64}\text{Cu}$  scan.

**Tumor volume.** As noted in the main text, tumor size was estimated from  $^{18}\text{F}$ -FDG tumor images. For most tumors (89 of 98 evaluated), the CT boundary was well approximated by the isocontour for a PET threshold setting = 50% of maximum. There were, however, instances in which relatively low tumor-to-background contrast required the threshold be as high as 80% in order to bring the isocontour within the tumor CT image.

## DISCUSSION

### Comparison with Clinical Investigations Using $^{89}\text{Zr}$ -trastuzumab in Metastatic Breast Cancer

Gebhart, et al., (2) qualitatively categorized patients according to the proportion of FDG-avid tumor load showing  $^{89}\text{Zr}$ -trastuzumab uptake > blood pool activity at 4 d post injection. Their findings (29% negative, 25% positive, 46% heterogeneous) are similar to our observations with  $^{64}\text{Cu}$ -DOTA-trastuzumab in HER2+ patients. On Day 2 (main text Fig. 1C), 3 HER2+ patients had average  $\text{SUV}_{\text{max}}$  ( $\langle \text{SUV}_{\text{max}} \rangle_{\text{pt}}$ ) that overlaps the  $\langle \text{SUV}_{\text{max}} \rangle_{\text{pt}}$  distribution for HER2- patients (27% negative), 2 HER2+ patients had all  $\text{SUV}_{\text{max}}$  values for individual tumors > any  $\text{SUV}_{\text{max}}$  from a HER2- patient (18% positive),

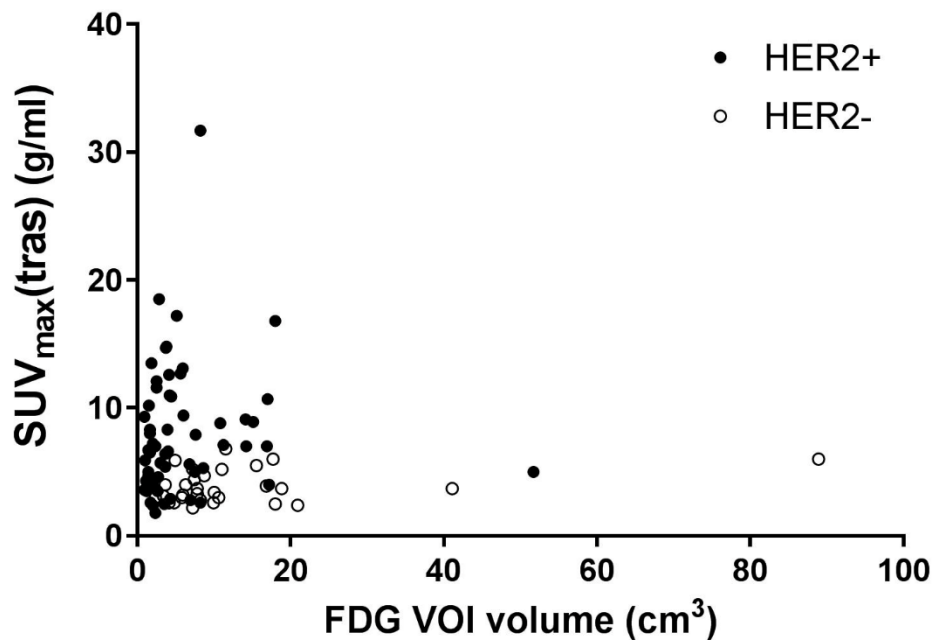


and 6 HER2+ patients had  $SUV_{max}$  distributions that partially overlap the HER2-  $SUV_{max}$  distribution (55% heterogeneous).

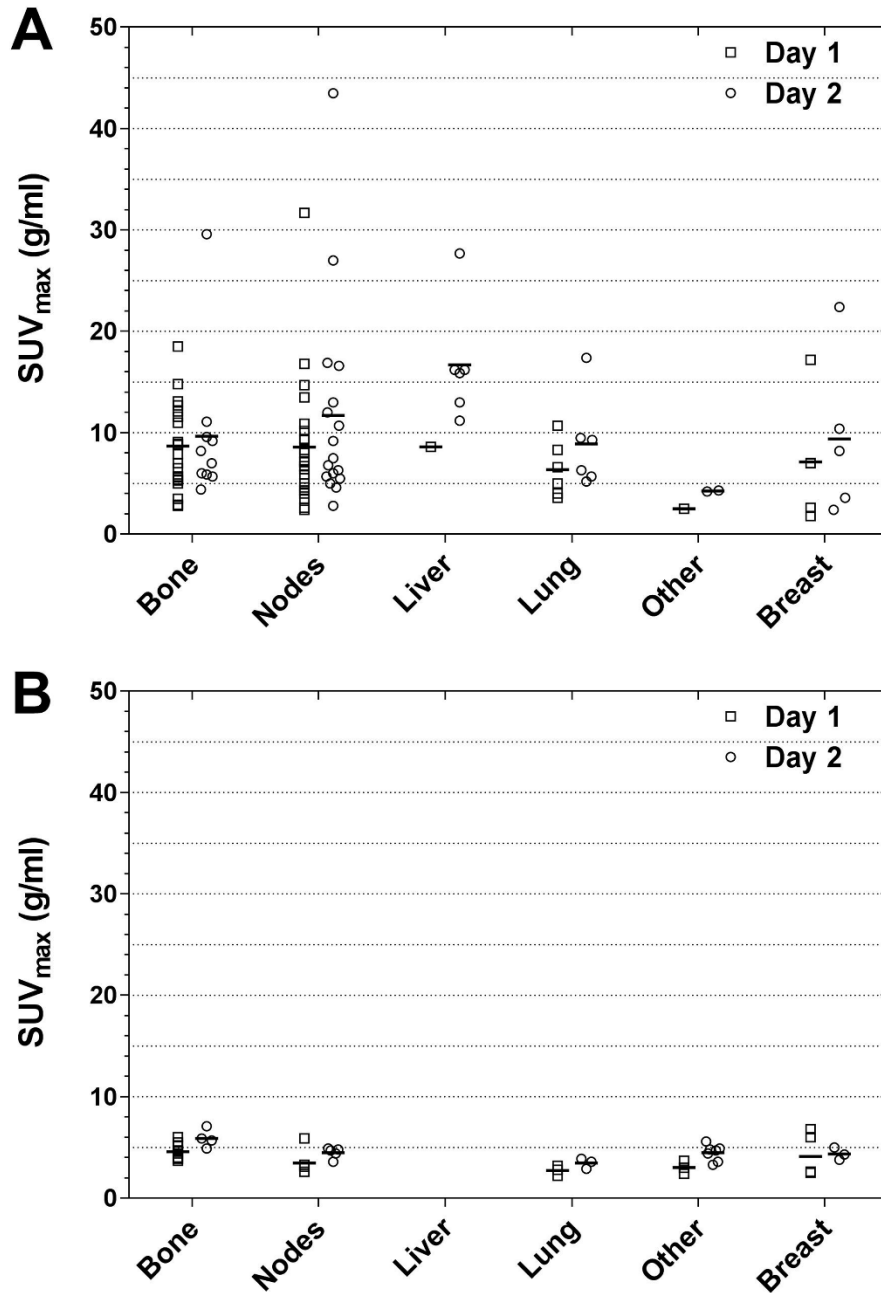
Ulaner, et al., (3) investigated tumor uptake of  $^{89}Zr$ -trastuzumab in 9 patients with HER2- primary tumors. Five of the patients had a “suspicious focus” of uptake on  $^{89}Zr$ -trastuzumab PET/CT performed 5 or 6 d post injection. Measured  $SUV_{max}$  in those lesions ranged from 4.6 to 9.7 g/mL; only the 2 with the lowest values (4.6 and 5.9 g/mL) were HER2+ on subsequent histopathology. These observations are consistent with ours (main text Fig. 1) both with regard to (i) the overlap of  $SUV_{max}$  distributions for nominally HER2+ and – disease and (ii) the absolute magnitude of  $SUV_{max}$ , given the difference in time between injection and scan for the 2 studies.

## REFERENCES

1. Boellaard R, Krak NC, Hoekstra OS, Lammertsma AA. Effects of noise, image resolution, and ROI definition on the accuracy of standard uptake values: a simulation study. *J Nucl Med* 2004;45:1519-1527.
2. Gebhart G, Lamberts LE, Wimana Z, et al. Molecular imaging as a tool to investigate heterogeneity of advanced HER2-positive breast cancer and to predict patient outcome under trastuzumab emtansine (T-DM1): the ZEPHIR trial. *Annals of Oncology* 2016;27:619-624.
3. Ulaner GA, Hyman DM, Ross, DS, et al. Detection of HER2-positive metastases in patients with HER2-negative primary breast cancer using  $^{89}Zr$ -Trastuzumab PET/CT. *J Nucl Med* 2016;57:1523-1528.



**SUPPLEMENTAL FIGURE 1.** Uptake of  $^{64}\text{Cu}$ -DOTA-trastuzumab (Day 1) vs. metabolic tumor size. The figure shows Day 1  $\text{SUV}_{\text{max}}(\text{tras})$  plotted against tumor size, measured in terms of  $^{18}\text{F}$ -FDG VOI volume. While the ranges of tumor size were similar for HER2+ and – patients, smaller tumors were proportionally more prevalent for the HER2+ than the HER2- group [volume (mean  $\pm$  SE)=  $6.2 \pm 1.0 \text{ cm}^3$  (n = 57) vs.  $13.1 \pm 3.1 \text{ cm}^3$  (n = 29);  $P < 0.001$ ] (Wilcoxon rank sum test). However, neither group showed significant dependence of  $\text{SUV}_{\text{max}}(\text{tras})$  on tumor size. Similar observations pertain to Day 2  $\text{SUV}_{\text{max}}(\text{tras})$ .



**SUPPLEMENTAL FIGURE 2.** Uptake of <sup>64</sup>Cu-DOTA-trastuzumab vs. lesion site. Shown are the SUV<sub>max</sub> data from (A) the HER2+ group (11 patients; number of lesions = 58 and 46 on Days 1 and 2, respectively) and (B) the HER2- group (7 patients; number of lesions = 29 and 28 on Days 1 and 2, respectively). Intra-patient means are represented by short horizontal lines. “Other” sites comprised pulmonary effusion for HER2+ patients and body

wall outside the breast for HER2- patients. There were no statistically significant differences among lesion sites for either HER2+ or HER2- patients on either day (F-test).